Published in final edited form as:
Adv Funct Mater. 2012 September 25; 22(18): 3793–3798. doi:10.1002/adfm.201200382.

Focal Infection Treatment using Laser-Mediated Heating of Injectable Silk Hydrogels with Gold Nanoparticles

Nikola Kojic[*], **Eleanor M. Pritchard**[*], **Hu Tao**[*], **Mark A. Brenckle**[*], **Jessica P. Mondia**, **Bruce Panilaitis**, **Fiorenzo Omenetto**[†], and **David L. Kaplan**[†]
Department for Biomedical Engineering, Tufts University, Medford, MA 02155, USA

Abstract

Medical treatment of subcutaneous bacterial abscesses usually involves systemic high-dose antibiotics and incision-drainage of the wound. Such an approach suffers from two main deficiencies: bacterial resistance to antibiotics and pain associated with multiple incision-drainage-wound packing procedures. Furthermore, the efficacy of high-dose systemic antibiotics is limited because of the inability to penetrate into the abscess. To address these obstacles, we present a treatment relying on laser-induced heating of gold nanoparticles embedded in an injectable silk-protein hydrogel. Although bactericidal nanoparticle systems have been previously employed based on silver and nitric oxide, they have limitations regarding customization and safety. The method we propose is safe and uses biocompatible, highly tunable materials: an injectable silk hydrogel and Au nanoparticles, which are effective absorbers at low laser powers such as those provided by hand held devices. We demonstrate that a single 10-minute laser treatment of a subcutaneous infection in mice preserves the general tissue architecture, while achieving a bactericidal effect - even resulting in complete eradication in some cases. The unique materials platform presented here can provide the basis for an alternative treatment of focal infections.

Keywords

silk hydrogel; bacterial infection; gold nanoparticle

1. Introduction

Management of infection in ischemic, avascular and necrotic tissues remains a major challenge due to the limitations of conventional systemic delivery of antibiotics. Drug penetration into abscesses is limited by both the lack of vascularity and the dense capsule wall, requiring high plasma concentrations to overcome the penetration barrier.[1–3] Conventional systemic delivery cannot meet this need due to dose-limiting tissue toxicities, particularly renal and liver complications.[4, 5] The difficulty of successfully treating abscesses with systemic antibiotic therapy is further compounded by high inter-individual variability in abscess permeability and the high variety of pathogens found in abscess fluid.[3] The rapid emergence of antibiotic-resistant infectious strains, such as methicillin-resistant *Staphylococcus aureus* (MRSA), and treatment delays associated with resistance-detection also highlight the importance of developing alternative infection treatments.[6–9] Because systemic antibiotic treatment alone is insufficient, the primary therapy for abscess management is incision and drainage followed by packing with non-degradable filler

[†]Corresponding authors: Fiorenzo Omenetto, David L. Kaplan, Tufts University, Department of Biomedical Engineering, 4 Colby St., Medford, Massachusetts 02155 U.S.A. Tel: 617-627-3251, Fax: 617-627-3231, fiorenzo.omenetto@tufts.edu, david.kaplan@tufts.edu.
[*]Authors contributed equally to this study

material to prevent wound collapse.[10, 11] Packing and removal of the filler-material is a painful process that may need to be repeated multiple times until the infection resolves. [12]

Thus, a treatment that obviates both the need to use antibiotics and the incision/drainage procedure may provide significant advantages. Treatments based on injectable nanoparticles (NP) (including nitric oxide and silver) have been proposed,[2, 13] but have significant limitations including safety concerns, poor biocompatibility, limited tunability and the need for a suitable carrier to ensure spatial stabilization at the injection site. Previous attempts to minimize gold nanoparticle (Au-NP) aggregation have included immobilization in various polymer hydrogels, including chitosan, alginate, methylcellulose and amphiphilic block copolymers, but these polymers lack the necessary biocompatibility and material structural tunability.[14] Though cancer cell and bactericidal effects of heating NPs have long been known, [15, 16] progress in thermotherapy has been limited by the lack of targeted delivery strategies.

Here we suggest an alternate treatment for focal infections based on laser-mediated heating of Au-NP suspended in an injectable and degradable silk hydrogel. The bactericidal procedure is as follows: the silk hydrogel and Au-NP composite is injected directly into the site of infection and a laser beam delivering 150 mW of incident green light (532 nm wavelength) is applied for 10 minutes. The wavelength of the incident light is absorbed by the nanoparticles and converted into heat (see the Supporting Information, Figure S1). This localized heat, in turn, has a bactericidal effect at the infection site without causing systemic side-effects.

To make such a platform feasible for future medical applications it must be: safe, effective, biocompatible, customizable, user friendly, and inexpensive. In order to satisfy these essential criteria we have selected a silk protein hydrogel, Au-NP, and a laser power that can be delivered with a handheld laser pointer.

Silk hydrogels exhibit excellent biocompatibility [17, 18] and tunable material properties. Silk gels degrade to non-toxic products in vivo and the degradation time of silk implants can be controlled from weeks to years.[19, 20] Silk can be processed entirely in water using mild, ambient conditions of temperature and pressure.[21] In particular, we have reported that the transition of silk solution to stable, physically crosslinked hydrogels can be induced without the addition of chemical crosslinking agents through sonication [22] or, as we describe here, vortexing.[23] Since gelation of the silk solution occurs after two hours (see Methods), other components like Au-NP can be mixed in prior to the onset of gelation, ensuring homogenous distribution throughout the hydrogel. Furthermore, the material properties of the silk hydrogel (e.g. stiffness) can be varied based on gelation time,[23] thus allowing control of spreading and localization of the injected hydrogel-NP composite. In addition to their photophysical properties, Au-NP are inert in vivo, non-toxic, and easy to synthesize.[14, 24]

2. Results and Discussion

The Au-NP silk hydrogel composite was first evaluated in vitro, followed by an in vivo study in mice. An in vitro setup was used to explore the parameter space of the material (Figure 1). Specifically, we assessed how power and duration of laser application affect the resulting temperature and bactericidal effect, and we probed the dynamics of nanoparticle heating for a variety of nanoparticle concentrations. The in vitro setup consisted of lawn cultures of bacteria grown on silk hydrogels with nanoparticles (Figure 1a–c). A laser beam (532 nm wavelength, diameter 5 mm) delivering a power of 450 mW was then directed over the central region of the gel for 15 minutes (Figure 1a). An IR camera was used during the time the laser was applied to measure the temperature response of the Au-NP dispersed inside the gel (Figure 1b). The heat map at the end of the laser treatment period shows a core

central region with a maximum of 59°C surrounded by zones with a sharp temperature gradient – the largest temperature difference being >30°C between the core and the outermost, unaffected areas of the gel (Figure 1b). Immediately after laser treatment the gel was placed in a 37°C incubator and then examined for bactericidal effects the next day. Following incubation and bacterial lawn formation, zones of clearance were observed where heat exposure had a bactericidal effect (the zones which remained clearly indicate the absence of bacteria, Figure 1a). Overlaying the IR temperature map and the image of the exposed lawn reveals that the zone-of-inhibition (ZOI) corresponds to the hottest core region, where temperatures were greater than 50°C (Figure 1c). ZOI only formed in the hydrogels with both Au-NP and laser exposure; Au-NP loaded hydrogel that is not exposed to laser, or empty silk hydrogel exposed to laser both fail to produce bacterial clearance (see the Supporting Information, Figure S2). For the same concentration of Au-NP in the gel (2.5x of arbitrary units – chosen in order to make the ZOI apparent upon visual inspection), we observe a roughly linear behavior for increased laser power and larger ZOI (Figure 1d), whereas shortening the laser exposure time decreases the ZOI (Figure 1e).

Another important parameter examined was the concentration of Au-NP in the hydrogel. By spanning a wide range of Au-NP concentrations from 1–40x (see Methods) we observed an asymptotic increase in the maximum temperature measured, ranging from 35–65°C (Figure 1f). The incident power and duration for these experiments was 150 mW and 10 minutes, respectively. The temporal evolution of the measured temperature showed that roughly 90% of maximum temperature was achieved after only 1 minute of laser exposure for every case of Au-NP concentration (Figure 1g). The concentration of Au-NP affects the color of the gel, ranging from a pink color (2.5x concentration, Figure 1a) to a darker purple (40x concentration, Figure 1h).

Prior to applying the system in vivo, we tested how heating would be affected by the presence of overlying tissue by using a slab of porcine meat and injecting the 40x Au-NP silk hydrogel at different depths (Figure 1h). At 2 mm below the surface the maximum temperature achieved was roughly 10°C above ambient and at 5 mm the temperature difference was only about 4°C. The incident beam used in both cases was 150 mW for 10 minutes, implying that at this low power the penetration depth for any considerable bactericidal effects is likely limited to the subcutaneous layer.

We performed in vivo studies with BALB/c mice infected with a subcutaneous injection of *S. aureus*. After 24 hours, infected wounds formed at the site of injection (Figure 2a). Each mouse (a total of six mice were used in the study) received four bacterial injections, which developed into four infected wounds treated with one of four experimental conditions: 1) untreated/non-lasered control infection, 2) injected with 40x Au-NP silk hydrogel and exposed to laser, 3) injected with silk hydrogel only (without Au-NP) and exposed to laser, 4) laser alone (without any gel/Au-NP injections) (Figure 2a,b). The power and duration of the laser treatment was 150 mW and 10 minutes, respectively. These parameters were chosen based on the in vitro results (Figure 1) in order to ensure bactericidal effects at the lowest laser power and exposure time. Increases in both power and duration are feasible and can enhance the overall bactericidal effect (Figure 1). During laser application, the temperature increase was recorded with the IR camera showing that the presence of Au-NP resulted in a maximum temperature of 55°C, whereas the exposure to the laser of the infected wound injected with only silk hydrogel caused the maximum temperature to reach a value of 40°C (Figure 2c). Applying the laser to the undisturbed infected wound yielded a maximum temperature of only 37°C (Figure 2c).

Following treatment, wounds were excised and homogenized using a mechanical homogenizer. The bactericidal effect was assessed by determining the number of colony

forming units (CFU) in the homogenate using standard plate counting methods (Table 1). CFU scaled with initial inoculate concentration, and no CFU were recovered from wounds receiving sterile broth (see the Supporting Information, Figure S3), suggesting that differences in CFU counts were attributable to treatment effects. To normalize for variability among the mice, CFU counts for each treatment modality were divided by the CFU count measured for the untreated wound and reported as a percentage (Figure 3a). The normalized CFU counts demonstrate that the wounds receiving laser treatment and Au-NP loaded silk hydrogel composite had a strong bactericidal effect, resulting in the CFU count being decreased to roughly 20% of control ($p<0.01$, Student t-test). The observed bacterial count reduction for this NP+Gel+Laser treatment group ranged from complete eradication (Figure 3b) to roughly 40% of the control wound (Figure 3a,b). The other two conditions, laser-exposed silk hydrogel with no NP (Gel+Laser) and infected wound exposed to laser (Laser), were not significantly different than the untreated control wound ($p>0.05$). As expected, the injected infection conditions (silk hydrogel +/− Au-NP) exhibited a wider range of variability than the other groups (Figure 3a) in large part due to the way the gel distributes subcutaneously and displaces each individual bacterial infection.

To assess the safety of the laser-induced heating, we examined histological slices of tissues surrounding the injected silk hydrogel loaded with Au-NP. Following injection of the hydrogel Au-NP composite, a laser beam delivering 150 mW for 10 minutes was applied. Histological sections then showed that the architecture of the neighboring tissues was undisturbed by the treatment (Figure 3c).

3. Conclusion

The results of our study indicate that focal heating of Au-NP injected into a subcutaneous infected wound is efficacious and safe, and bypasses the need for antibiotics. Based on the tunability demonstrated in our in vitro experiments we anticipate treatment efficacy could be further increased. In particular, the control over silk hydrogel properties, Au-NP concentration, laser exposure duration, and laser power provides the ability to determine the optimal, case-specific treatment scenario. The in vivo results demonstrate bacterial reduction after one round of laser-exposure, but we also anticipate that once the hydrogel carrier is injected, multiple courses of focal heating could be administered as needed. Gold nanoparticles provide safe focal heating. The silk hydrogel is unique in this application as it provides a biocompatible, biodegradable, tunable carrier, preventing nanoparticle aggregation and ensuring spatial stabilization at the injection site. Moreover, the procedure is straightforward, involving laser powers that can be delivered by a hand held device, and uses inexpensive, non-toxic biomaterials.

This study can serve as a basis for further investigations aimed at optimizing the system for a range of wound sizes and infection types, as well as the possibility of repeated treatments for intractable cases. In addition, the treatment platform described here would be effective against a wide range of bacteria, including antibiotic-resistant strains and, due to this broad-specificity, could be initiated without waiting for screening results. We anticipate this composite delivery system could be extended to other clinical needs, especially localized hyperthermia-based cancer treatment and triggered or inducible drug delivery. Finally, based on our recent demonstration of silk-fiber optics,[25] a particularly intriguing option would be to use the approaches described here to access deep infection sites in the body. This would be particularly important for infections in sites which are difficult to reach with systemic antibiotic delivery, such as bone infections [26] or brain abscesses.[27]

4. Experimental Section

Materials

The bacteria strains used were *Escherichia coli* ATCC 25922 and *Staphlococcus aureus* ATCC 25923 (American Type Culture Collection, Manassas, VA). Bacterial culture dishes, BD brand Luria-Bertani broth, Miller, BD brand Luria-Bertani agar, Miller, Tryptic Soy broth and Tryptic Soy agar were purchased from Fisher Scientific (Pittsburgh, PA).

Gold nanoparticle fabrication

Gold nanoparticles were fabricated by boiling 20 ml of 1.0 mM gold chloride ($HAuCl_4$, Sigma-Aldrich) and then adding 2 ml of 1 % sodium citrate (Sigma-Aldrich), while rapidly stirring the mixture for 15 min. The solution was then gradually cooled to room temperature, and was filtered by 0.22 μm filter paper. This gives a gold nanoparticle solution with a concentration of ~3.5 nM and an average particle size of ~13 nm, which was further concentrated to ~17.5 nM (termed 80x concentration of arbitrary units) by centrifuging for 20 min at 4°C, with a RCF of 11930 g.

Silk hydrogel preparation

Silk fibroin aqueous solutions were prepared as previously described [28]. Briefly, *Bombyx mori* cocoons were boiled for 60 min in an aqueous solution of 0.02 M sodium carbonate and then rinsed thoroughly with deionized water. After overnight drying, the silk fibroin was dissolved in an aqueous solution containing 9.3M LiBr at 60°C for 6 hours. The solution was dialyzed against deionized water using Slide-a Lyzer dialysis cassettes (MWCO 3,500, Pierce, Rockford, IL) for two days to remove the residual salt. The final concentration of the silk fibroin was roughly 6 wt %. This stock silk solution was then further diluted with deionized water down to 2 wt%, and 1 mL of 2 wt% solution was mixed for 7 minutes at 3,200 rpm using a vortexer (Fisher Scientific, Hampton, NH) to induce silk self-assembly and hydrogelation. Immediately after vortexing, while still in the liquid state, the addition of bacteria, Au-NP, and/or deionized water decreased the final silk concentration to ~1 wt%. This final composite solution was placed in a 37°C incubator for 2 hours resulting in the transition to a gel state.

Bacteria culture

Luria Bertani (LB) and Tryptic Soy Broth were aliquoted into 100 mm diameter Fisherbrand cell culture plates (15–20 mL per plate). Lyophilized bacteria cultures were reconstituted and expanded according to instructions provided by ATCC. To test susceptibility, liquid cultures were grown for 18–24 hours to an optical density (OD_{600}) between 0.8 and 1 (corresponding to a viable count of approx. 10^7–10^8 CFU/mL).

In vitro zone of inhibition testing

Antibacterial effect in vitro was estimated based on the principle of the Kirby-Bauer Susceptibility Test where antibacterial effect is assessed by comparing zones of clearance in bacterial lawns. Vortexed silk hydrogel, *S. aureus* overnight culture and a suspension of gold nanoparticles were mixed in a 2:1:1 volumetric ratio and the silk hydrogel was allowed to complete gelation. Hydrogels were then exposed to laser light of varying duration and power and incubated overnight at 37°C to allow lawn growth. After 24 hours the zone of inhibition (ZOI) was measured using Image J image analysis software.

Subcutaneous S. aureus infection in vivo studies

Male BALB/c mice weighing 20–25 g were shaved on the back and depilated with Nair (Carter-Wallace Inc., New York, NY). Mice were anesthetized with an IP injection of

ketamine/xylazine cocktail (90 mg/kg ketamine, 10 mg/kg xylazine) for surgery and infection. The operative area of skin was cleaned with alcohol, and subcutaneous injections containing live bacteria were given at four different sites on the shaved back of each animal. Each 50 μL injection contained 1 x 10^6 colony forming units (CFU) of *S. aureus*. After 24 hours, raised bumps were observed at the four injection sites. Each animal (N=6) received four treatments: 1) untreated/unlasered control infection, 2) injected with 100 μL of 40x Au-NP silk hydrogel and exposed to laser, 3) injected with 100 μL silk hydrogel only (without Au-NP) and exposed to laser, 4) laser alone (without any gel/Au-NP injections). During the 10 minutes of laser application the animals were under anesthesia.

At specified times following laser treatment, animals were anesthetized and the infected tissue and surrounding tissues were excised and transferred to sterile 50-ml Falcon tubes containing 10 ml of sterile saline for further processing. The mice were then euthanized by carbon dioxide asphyxiation. All animal studies were conducted under protocols reviewed and approved by the Tufts University IACUC.

Excised tissue samples were homogenized using a T25 basic Ultra Turrax mechanical homogenizer (IKA Works, Inc., Wilmington, NC). Bacteria in the homogenate were estimated by standard plate count methods [29,30]. Colonies were counted after 24 hr of incubation at 37°C. The bacterial count was expressed as the number of colony forming units (CFU) per wound. To normalize for variability among the mice, CFU counts for each treatment modality were divided by the CFU count measured for the untreated wound and reported as a percentage.

Histology

To assess the safety of our heating procedure, we examined histological slices of tissues surrounding the injected silk hydrogel loaded with Au-NP. Samples were dehydrated through a series of graded alcohols, embedded in paraffin and sectioned at 10 μm thickness. Sections were stained with hematoxylin and eosin (H&E).

Supplementary Material

Refer to Web version on PubMed Central for supplementary material.

Acknowledgments

We thank the NIH (EB002520, AR005593, AR061988). Supporting Information is available online from Wiley InterScience or from the author.

References

1. Gerding DN, Kozak AJ, Peterson LR, Hall WH. Antimicrob Agents Chemotherapy. 1980; 17:1023–1029.
2. Han G, Martinez LR, Mihu MR, Friedman AJ, Friedman JM, Nosanchuk JD. Plos One. 2009; 4
3. Sauermann R, Karch R, Langenberger H, Kettenbach J, Mayer-Helm B, Petsch M, Wagner C, Sautner T, Gattringer R, Karanikas G, Joukhadar C. Antimicrob Agents Chemotherapy. 2005; 49:4448–4454.
4. Price JS, Tencer AF, Arm DM, Bohach GA. J Biomed Mater Res. 1996; 30:281–286. [PubMed: 8698690]
5. Ruszczak Z, Friess W. Adv Drug Delivery Rev. 2003; 55:1679–1698.
6. Englander L, Friedman A. J Clin Aesthet Dermatol. 2010; 3:45–50. [PubMed: 20725551]
7. Louie L, Matsumura SO, Choi E, Louie M, Simor AE. J Clin Microbiol. 2000; 38:2170–2173. [PubMed: 10834971]

8. White RJ, Cutting K, Kingsley A. Ostomy Wound Management. 2006; 52:26–58.
9. Nordmann P, Poirel L, Toleman MA, Walsh TR. J Antimicrob Chemotherapy. 2011; 66:689–692.
10. Fitch MT, Manthey DE, McGinnis HD, Nicks BA, Pariyadath M. New Eng J Med. 2007; 357:E20–U25. [PubMed: 17989377]
11. Stearne LET, Buijk SL, Mouton JW, Gyssens IC. Antimicrob Agents Chemotherapy. 2002; 46:3712–3718.
12. O'Malley GF, Dominici P, Giraldo P, Aguilera E, Verma M, Lares C, Burger P, Williams E. Acad Emergency Med. 2009; 16:470–473.
13. Kumar A, Vemula PK, Ajayan PM, John G. Nat Mater. 2008; 7:236–241. [PubMed: 18204453]
14. Marsich E, Travan A, Donati I, Di Luca A, Benincasa M, Crosera M, Paoletti S. Coll Surf B-Biointerfaces. 2011; 83:331–339.
15. Doherty CB, Doherty SD, Rosen T. J Amer Acad Derm. 2010; 62:909–927. [PubMed: 20466169]
16. Lee ES, Caldwell MP, Talarico PJ, Kuskowski MA, Santilli SM. Wound Repair Regen. 2000; 8:562–566. [PubMed: 11208184]
17. Leal-Egana A, Scheibel T. Biotech Appl Biochem. 2010; 55:155–167.
18. Meinel L, Hofmann S, Karageorgiou V, Kirker-Head C, McCool J, Gronowicz G, Zichner L, Langer R, Vunjak-Novakovic G, Kaplan DL. Biomaterials. 2005; 26:147–155. [PubMed: 15207461]
19. Horan RL, Antle K, Collette AL, Huang YZ, Huang J, Moreau JE, Volloch V, Kaplan DL, Altman GH. Biomaterials. 2005; 26:3385–3393. [PubMed: 15621227]
20. Wang Y, Rudym DD, Walsh A, Abrahamsen L, Kim HJ, Kim HS, Kirker-Head C, Kaplan DL. Biomaterials. 2008; 29:3415–3428. [PubMed: 18502501]
21. Vepari C, Kaplan DL. Prog Polymer Sci. 2007; 32:991–1007.
22. Wang XQ, Kluge JA, Leisk GG, Kaplan DL. Biomaterials. 2008; 29:1054–1064. [PubMed: 18031805]
23. Yucel T, Cebe P, Kaplan DL. Biophys J. 2009; 97:2044–2050. [PubMed: 19804736]
24. Ghosh P, Han G, De M, Kim CK, Rotello VM. Adv Drug Delivery Rev. 2008; 60:1307–1315.
25. Parker ST, Domachuk P, Amsden J, Bressner J, Lewis JA, Kaplan DL, Omenetto FG. Adv Mater. 2009; 21:2411.
26. Nandi SK, Mukherjee P, Roy S, Kundu B, De DK, Basu D. Mat Sci Eng C-Mat Biol App. 2009; 29:2478–2485.
27. Raza MW, Shad A, Pedler SJ, Karamat KA. J Coll Physicians Surg Pak. 2005; 15:165–167. [PubMed: 15808097]
28. Sofia S, McCarthy MB, Gronowicz G, Kaplan DL. J Biomed Mater Res. 2001; 54:139–148. [PubMed: 11077413]
29. Georgiade NG, Lucas MC, Osterhou S. Amer J Clin Path. 1970; 53:40–42. [PubMed: 4903063]
30. Saymen DG, Hill EO, Holder IA, Nathan P, Macmilla BG. Appl Microbiol. 1972; 23:509–514. [PubMed: 4623279]

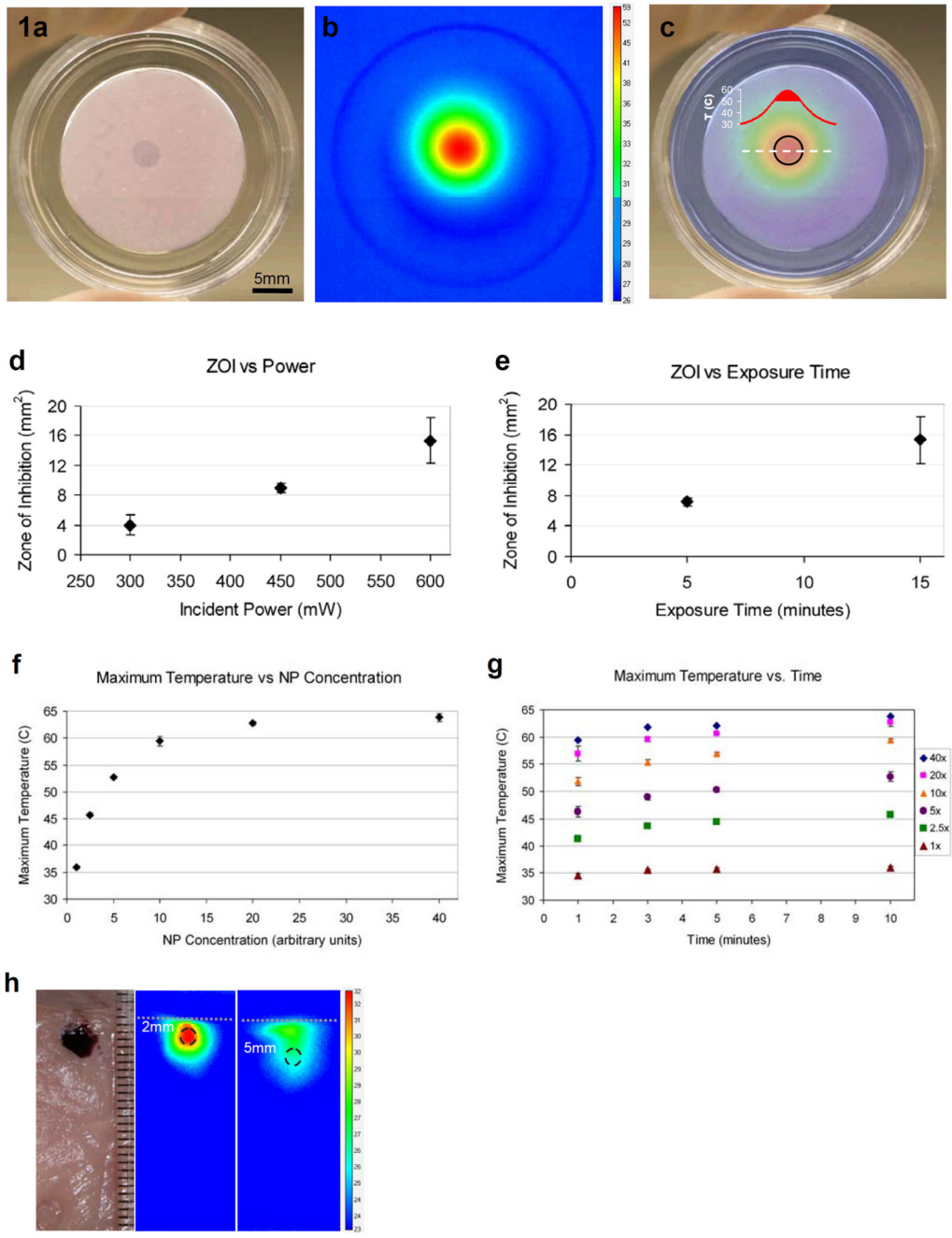

Figure 1.

In vitro tests of the silk hydrogel Au-NP composite. a) Bactericidal effects observed in the central clear region where laser was applied (450 mW for 15 minutes, NP concentration 2.5x). Central clear zone, termed zone of inhibition (ZOI), indicates lack of bacterial presence, whereas surrounding turbid area represents a bacterial lawn. b) IR camera images of the temperature map at the end of laser application. Temperature scale bar in °C. c) Overlay of a) and b). Black circle: ZOI; graph: temperature profile of dashed white line, solid red shading (>50°C) corresponds to ZOI region. d) ZOI for various laser power (exposure time 15 minutes, NP concentration 2.5x). e) ZOI for various durations of laser exposure (600mW, 2.5x NP). f) Maximum temperature achieved for various NP

concentrations (laser power 450mW, exposure time 10 minutes) and the corresponding g) maximum temperatures for several laser exposure times. h) Edge-on view of a slab of porcine meat injected with NP+Gel (40x concentration) at a depth of 2 mm below the surface. Laser (150 mW) was applied for 10 minutes to the surface layer directly above injection sites. Temperature maps for 2 mm and 5 mm cases at the end of exposure to laser. Ruler next to slab in mm, dashed white line represents slab surface, black dashed circles correspond to injection sites, temperature scalebar in °C.

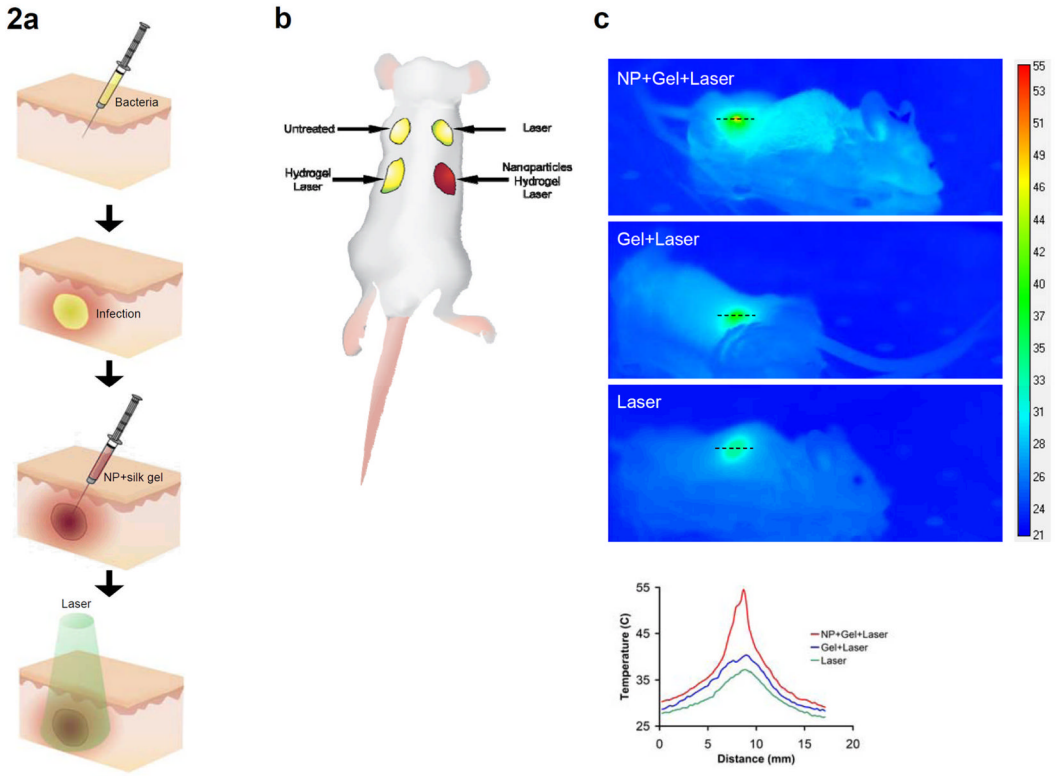

Figure 2.

In vivo experimental schematic and temperature mapping. a) Schematic of subcutaneous injection procedure. Infection was allowed to fester for 24 hours after bacterial injection. b) Layout of the 4 infection sites (red represents color of gel+NP composite). c) Temperature map of the 3 infection sites receiving laser treatment (power 150mW, exposure time 10 minutes). NP concentration was 40x. Graph: temperature profiles corresponding to dashed black lines. Scalebar in °C.

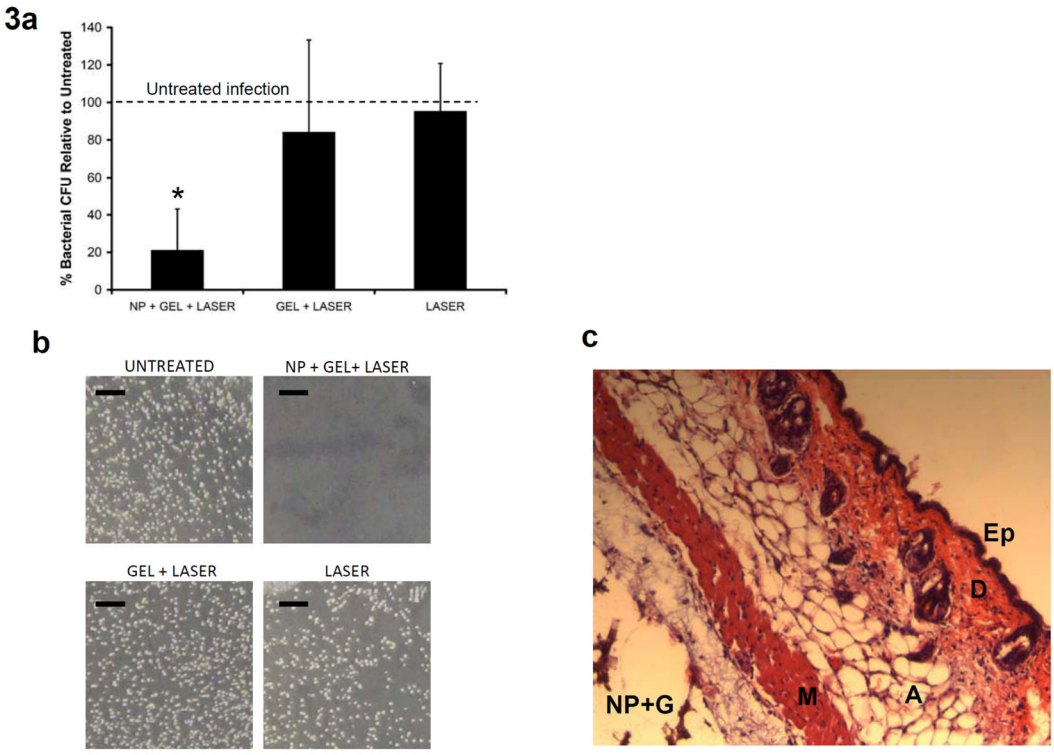

Figure 3.

In vivo treatment results and histology. a) Graph of percent bacterial CFU normalized to the untreated infection. The 3 groups represent infection sites receiving laser treatment (150 mW for 10 minutes). Star (*) indicates significant difference from untreated infection ($p<0.01$, Student t-test). NP concentration=40x, N=6 mice. b) Images of actual bacterial CFUs obtained from the 4 wound sites of mouse # 3 (see Table 1) showing infection eradication at the laser-treated NP+Gel wound site. c) Histology (H&E stain) of the NP+Gel site, indicating that the general tissue architecture is preserved after laser treatment. Ep: epidermis, D: dermis, A: adipose tissue, M: muscle, NP+G: Au-NP in silk hydrogel.

Table 1

Individual wound treatment responses for the 6 mice used in the study. All groups except “Untreated” received laser treatment (150 mW for 10 minutes). Units are in 10^6 Colony Forming Units (CFU) per wound.

	# 1	# 2	# 3	# 4	# 5	# 6
Untreated	103.3	251.7	428.0	16.1	16.5	9.9
NP + Gel + Laser	6.4	36	0.58	9.2	1.9	3.8
Gel + Laser	42.0	221.3	233.7	28.0	8.5	9.7
Laser	96.7	265.3	568.0	15.7	14.7	5.4